Cold Rolling Texture of Heavy Rolled 50 Pct Ni-Fe Thin Sheets

Cold Rolling Texture of Heavy Rolled 50 Pct Ni-Fe Thin Sheets*

Haruo KATO and Eihachiro TANAKA

The Research Institute for Iron, Steel and Other Metals

(Received February 17, 1969)

Synopsis

In order to clarify the cold rolling texture of heavy rolled ultra-thin sheets of 50 pct Ni-Fe alloy, the effect of extremely high reduction and final thickness of sheets on the texture and the variation of textures through the thickness have been investigated.

It has been recognized that the rolling textures of this alloy indicate to be copper-type up to this time. However, it could not be simply described as copper-type and show the peculiar textures under such an extreme rolling condition.

The results obtained are summarized as follows:

(1) The center textures up to 99.4 pct reduction and in the thicker sheets than 20 μ in thickness show the sharp copper-type.

(2) After much higher reduction than 99.4 pct, {110}⟨112⟩ component decreases and (112)⟨111⟩ component increases and such tendency is more remarkable in thinner sheets and the surface layer.

(3) After much higher reduction than 99.9 pct, weak {110}⟨335⟩ and {110}⟨100⟩ component increase slowly with increase of reduction and is stronger in the surface layer.

(4) Very weak {100}⟨001⟩ component exists in deformed matrix, but after heavy reduction more than 99.4 pct and in thinner sheets than 20 μ, this component decreases still more.

(5) The integrated intensity of {100} ⟨001⟩ in deformed matrix corresponds to numbers of {100}⟨001⟩ in the recrystallized nuclei.

From the above results the mechanisms of texture formation in ultra-thin sheets are discussed.

I. Introduction

In general, fcc metals and alloys develop, by heavy rolling, either or two types of texture, classified for convenience as copper-type and brass-type.

Current theories on the mechanism of texture transition in fcc metals, the copper-type→the brass-type, can be summarized as follows:

(1) Texture transition due to mechanical twining.[1]

(2) Texture transition caused by cross slip.[2],[3]

(3) Texture transition caused by non-octahedral slip.[4]

---

* The **1393rd** report of the Research Institute for Iron, Steel and Other Metals. Presented at the general meeting of the Japan Institute of Metals at Sendai, September, 1968. To be published in the J. Japan Inst. Metals, **33** (1969), No. 3 (in Japanese).

(1) G. Wassermann, Z. Metallk., **54** (1963), 61.

(2) I.L. Dillamore and W.T. Roberts, Acta Met., **12** (1964), 281.

(3) R.E. Smallman and D. Green, Acta Met., **12** (1964), 145.

(4) F. Haessner, Z. Metallk., **54** (1963), 98.

(4) Texture transition caused by dislocation interraction.[5]

While considerable data[6]~[9] have been published on the heavy rolling texture in 50 pct Ni-Fe alloy, the limit of cold rolling reduction was at most 99.5 pct and only very little study has been made on the effect of interaction between the rolls and the rolled materials, especially, in ultra-thin sheets.

The intensity in the recrystallized cube texture decreased remarkably for the the heavy rolled and ultra-thin sheets, as reported previously,[10] and the cause of this inferiority in cube texture has not been explained clearly.

The present investigation was undertaken to study the effect of cold rolling reduction and thickness on texture transition in the case of specimens of ultra-high reduction and ultra-thin thickness and the variation of textures through the thickness.

II. Experimental method and specimens

1. Specimens

The Ni-Fe alloy used in the experiment was vacuum melted in a high frequency induction furnace. The 50 kg ingots containing 0.02 pct C, 0.002 pct P, 0.24 pct Mn, 0.40 pct Co and 42.82 pct Ni were forged, hot rolled and then cold rolled to strips of 0.15~0.006 mm in thickness, as shown in Table 1.

Table 1. Rolling schedule of specimens.

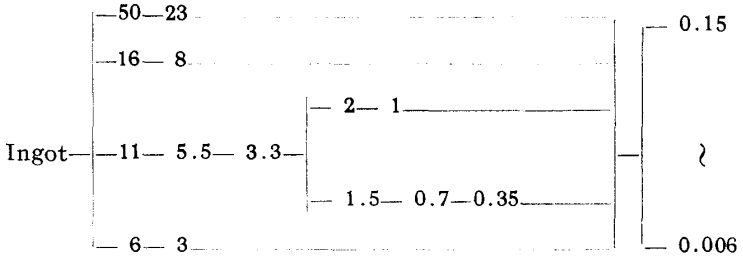

(unit : mm)

Each intermediate annealing during cold rolling was done at 850°C for 3 hr in hydrogen, the grain sizes of the plates just before finishing rolling were 0.03~0.06 mm in diameter and the effect of difference in ingots on working process was not observed.

The sheets were reversely rolled to 3 mm with 2-Hi mill, rolled to 0.15 mm with 4-Hi mill and the thickness less than 0.15 mm were rolled with 20-Hi mill which has 300, 150 and 6 mm dia. rolls. The draught per pass was about 10 pct and the total reductions of specimens were from 86.5 to 99.97 pct.

(5) Y.C. Liu, Trans. Met. Soc. AIME, **230** (1964), 656.
(6) G. Sachs and J. Sprentnak, Met. Tech., 1940, T.P. 1143.
(7) E. Schmid and H. Thomas, Z. Physik, **130** (1951), 293.
(8) M.F. Litlman, Trans. Met. Soc. AIME, **206** (1956), 593.
(9) S. Spachner and W. Rostoker, J. Metals, **7** (1955), 921.
(10) E. Tanaka and H. Kato, J. Japan Inst. Metals, **21** (1957), 651; **22** (1958), 30.

2. Texture determination

The development of rolling textures was studied by examining complete pole figures determined from the (111) and (200) reflection using Cu-K_α and Fe-K_α radiation. Specimens electrically thinned from both surfaces to 0.002 mm were used to obtain the textures of the center layer, while specimens thinned from one surface of the strips to $0.001 \sim 0.002$ mm were used to obtain the surface textures.

III. Experimental results

Typical (111) pole figures of heavy rolled 50 pct Ni-Fe alloy thin sheets with reductions from 90 to 99.9 pct are shown in Fig. $1 \sim$ Fig. 5. The pole figures in the center layer are seen to represent a continuous development toward the final copper-type texture, (110) $[\bar{1}12]$ and (112) $[\bar{1}\bar{1}1]$, up to 99.4 pct reduction, with increasing reduction, as shown in Fig. 1 and Fig. 2, respcectively.

With thinning from 50 to 6 μ for the same 99.4 pct reduction, so-called sharp copper-type texture begins to change, that is, the orientation of (110) $[\bar{1}12]$ spread in orientation and rotates to the (112) $[\bar{1}\bar{1}1]$ orientation, as shown in Fig.2 and Fig. 3. And these tendency, as mentioned above, appears to increase with increasing reduction, as shown in Fig. 4.

The general features of the textures developed at the various sections through the strip thickness in heavy rolled thin sheets are as follows:

The (112) $[\bar{1}\bar{1}1]$ orientation increase greatly, (110) $[\bar{1}12]$ orientation decreases

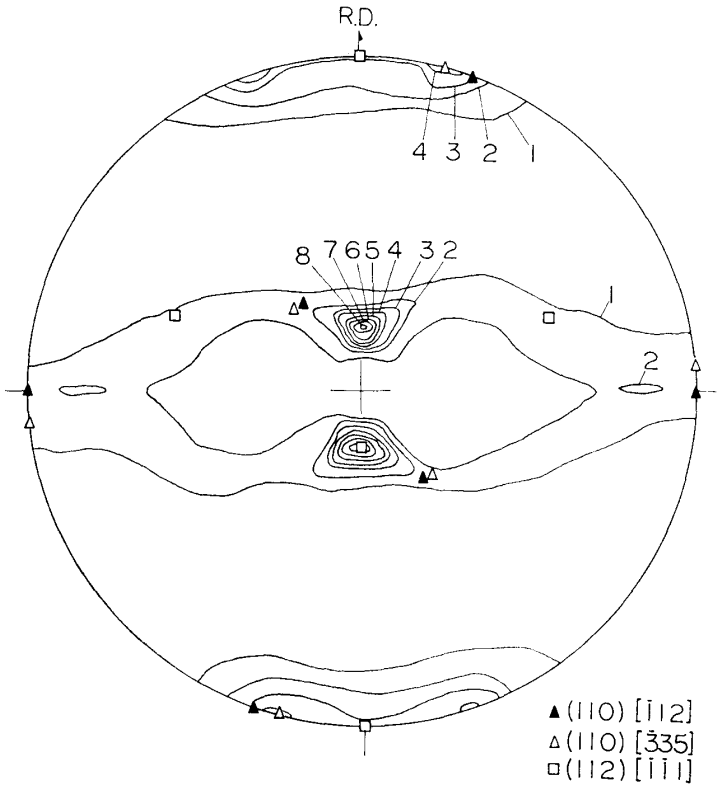

Fig. 1. (111) pole figure for rolled 90 pct reduction 35 μ thickness. (center layer)

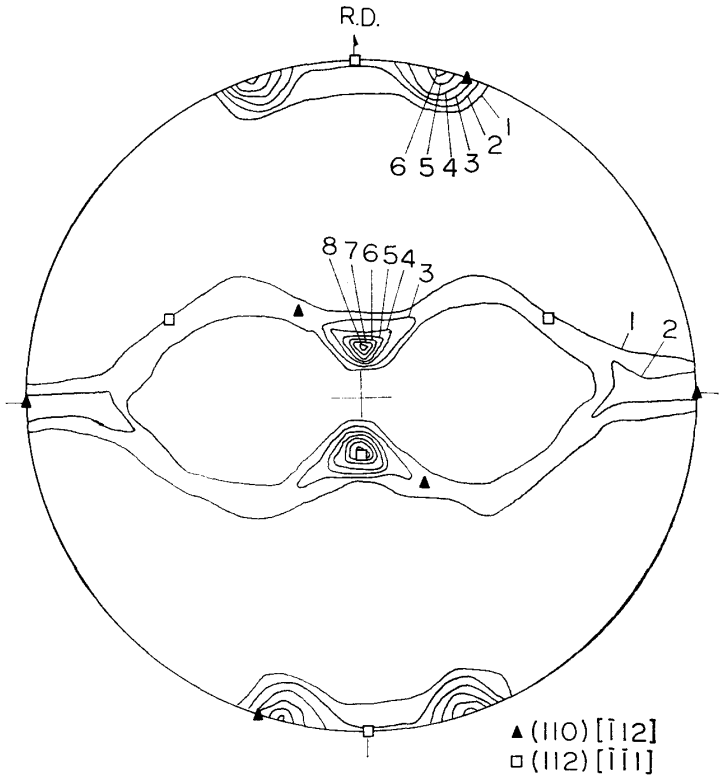

Fig. 2. (111) pole figure for rolled 99.4 pct reduction, 20 μ thickness. (center layer)

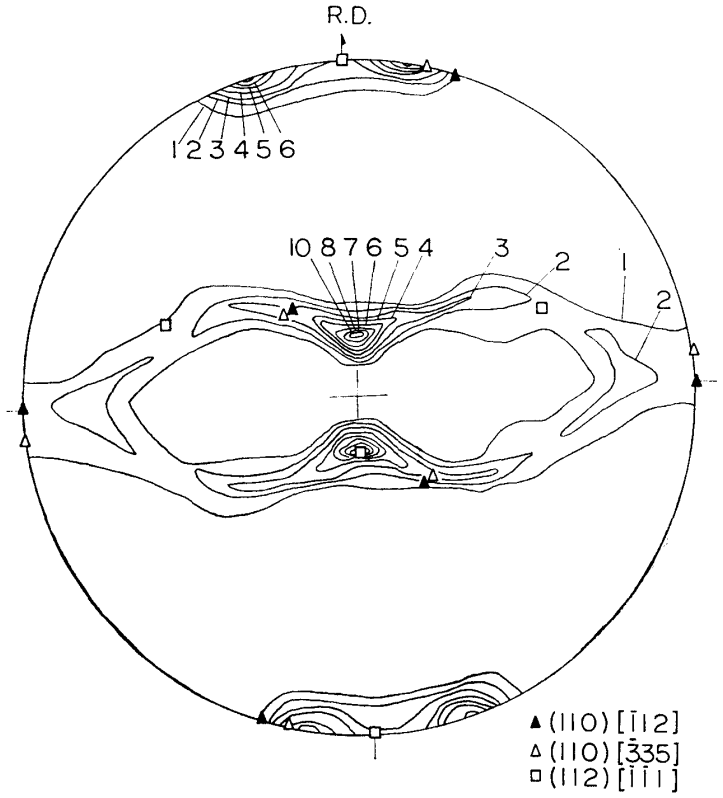

Fig. 3. (111) pole figure for rolled 99.4 pct reduction, 6 μ thickness. (center layer)

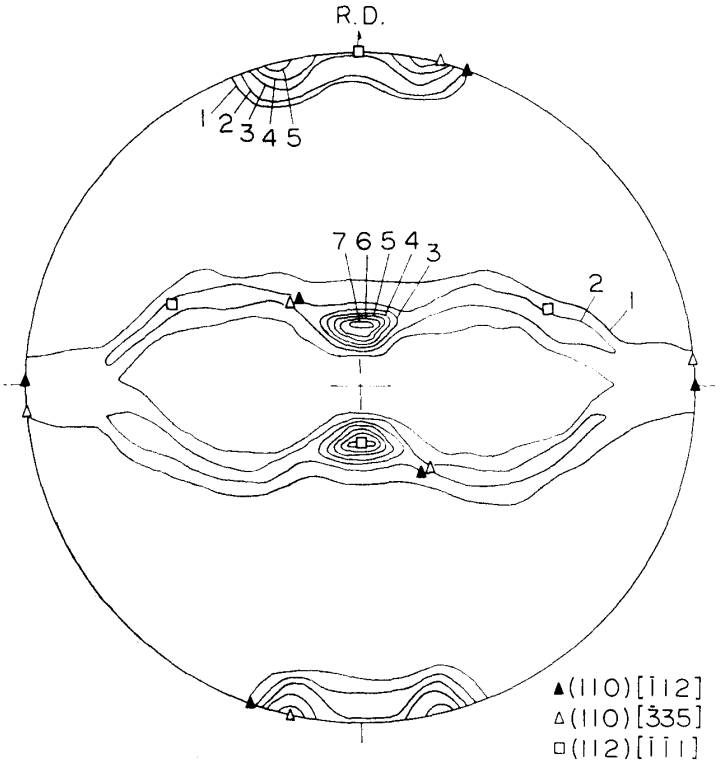

Fig. 4. (111) pole figure for rolled 99.9 pct reduction, 7 μ thickness. (center layer)

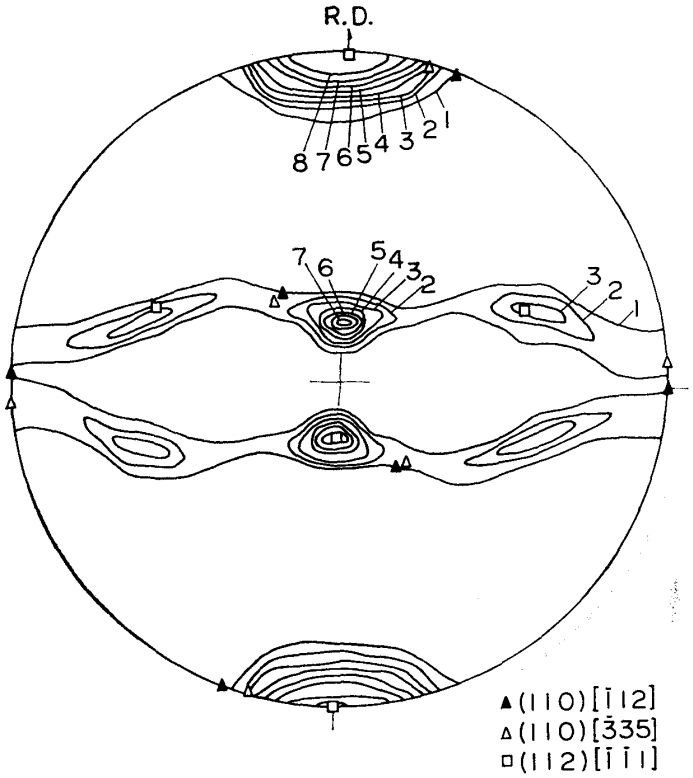

Fig. 5. (111) pole figure for rolled 99.9 pct reduction, 7 μ thickness. (surface layer)

and (110) [$\bar{3}35$] and (110) [001] orientation begin to develop, in the typical specimen which rolled to 7 μ in thickness with 99.9 pct reduction, as shown in Fig. 4 and Fig. 5.

Fig. 6 shows the effect of cold rolling reductions in the center layer on the variation of the intensity distribution along the peripheral circle of (111) diffraction

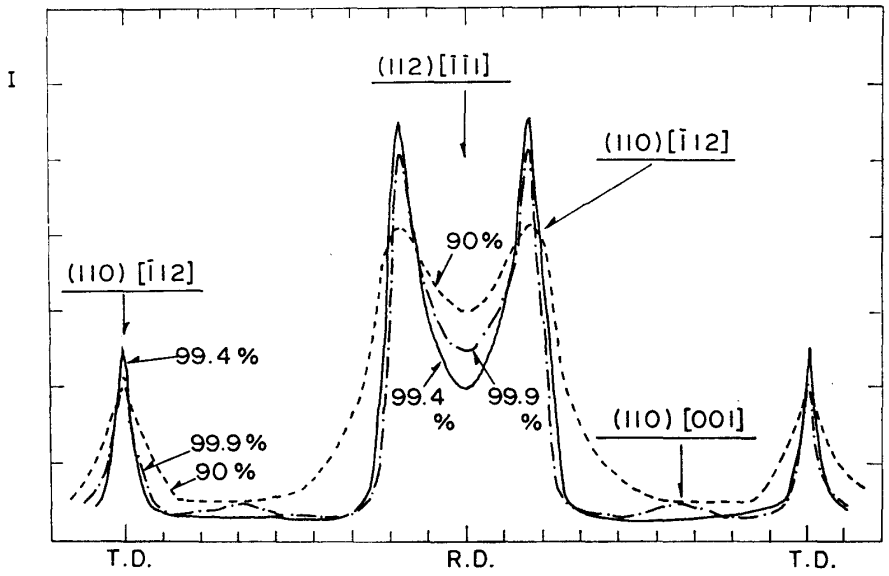

Fig. 6. Effect of cold rolling reduction on the variation of intensity distribution along the peripheral circle of (111) diffraction line from rolled 20~30 μ thickness.

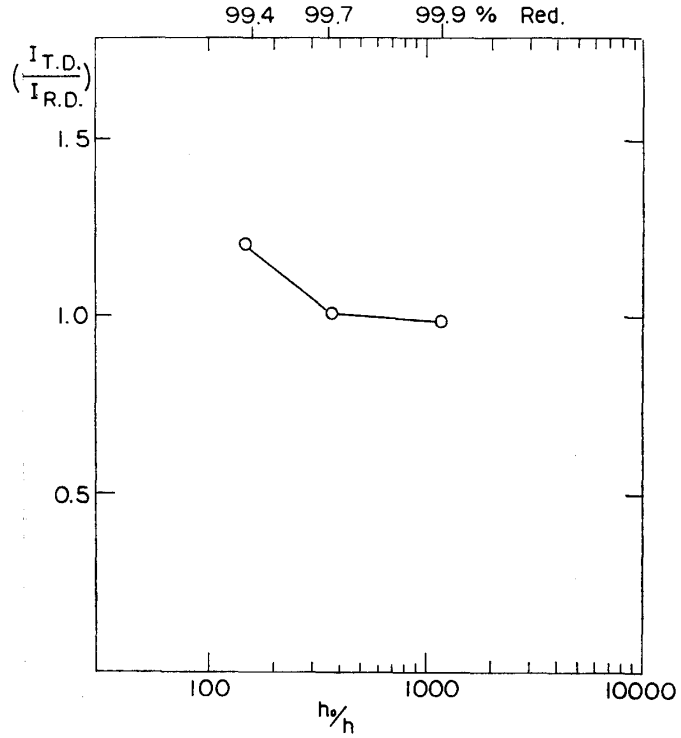

Fig. 7. Effect of cold rolling reduction on ($I_{T.D.}/I_{R.D.}$) for reduced 20 μ thickness (center layer).

line, in the specimens rolled $20 \sim 30\ \mu$ in thickness, in which (112) [$\bar{1}\bar{1}1$] intensity, $I_{R.D.}$, decreases up to 99.4 pct from 90 pct reduction and again increases with increasing reduction, but (110)[112] *vice versa*. From the above results, the relation of the intensity ratio, $I_{T.D.}/I_{R.D.}$, with the reduction for $20\ \mu$ in thickness, is shown in Fig. 7 and the ratio decreases little by little with increasing reduction which is much higher than 99.4 pct, that is, (110) [$\bar{1}$12] component decreases and (112) [$\bar{1}\bar{1}$1] component increases.

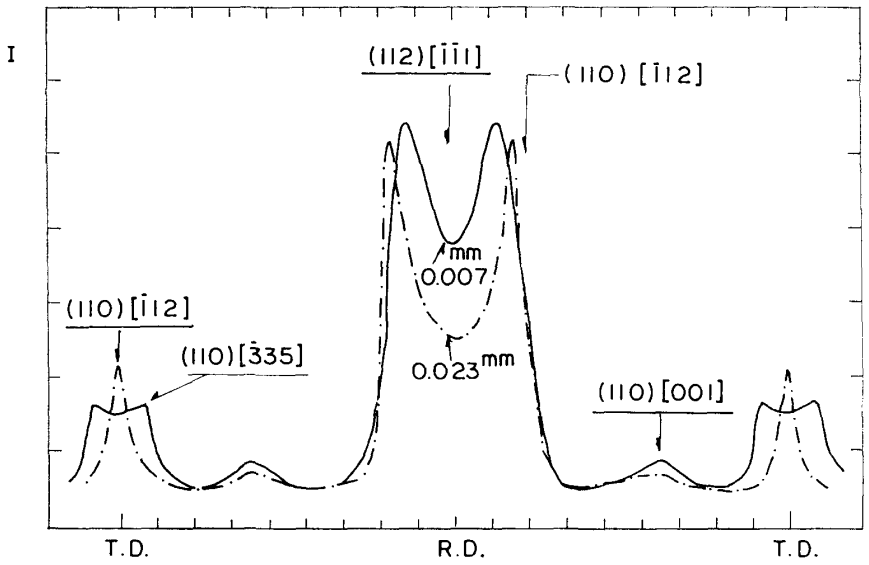

Fig. 8. Effect of thickness on the variation of intensity distribution along the peripheral circle of (111) diffraction line for rolled 99.9 pct reduction (center layer).

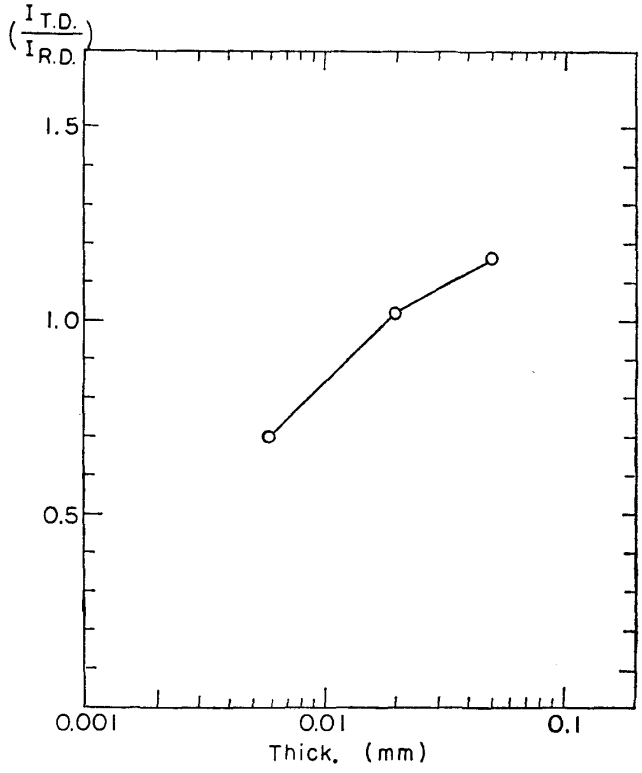

Fig. 9. Effect of thickness on ($I_{T.D.}/I_{R.D.}$) for rolled 99.4 pct reduction (center layer).

Fig. 8 shows the effect of thickness on the variation of intensity distribution in the center layer of specimens along the peripheral circle of (111) diffraction line for the specimens rolled 99.9 pct reduction. As seen from the figure, (112) [$\bar{1}\bar{1}1$] component develops and (110) [$\bar{1}12$] component diminishes greatly for the specimens of 7 μ, compared with those of 23 μ in thickness rolled 99.9 pct reduction. From the result, it appears that the thickness has more largely effect on the orientation rotation from (110) [$\bar{1}12$] to (112) [$\bar{1}\bar{1}1$] component than the reduction.

This tendency is conspicuous in the specimens less than 10 μ in thickness, as shown in Fig. 9. And it develops an additional texture component that the change in orientation appears to be characterized mainly by a rotation in the counter-clockwise direction around the normal to the (110) rolling plane, presented (110) [$\bar{3}35$] component, and also, a rotation in the clokwise direction that can be described as (110) [001]. Fig. 10 shows the effect of cold rolling reduction and the thickness in the specimens rolled from 8 mm in thickness on the breadth of half-maximum intensities at the position of transverse direction (T.D.) of (111) diffraction line, expressed a rotation in the counter-clockwise direction around the normal to the (110) rolling plane. The breadth of half-maximum intensities, that is, an angle of rotation increases by increasing reduction and thinning thickness.

Fig. 11 shows the effect of the surface layer on the variation of intensity distribution along the peripheral circle of (111) diffraction line for rolled 99.9 pct sheet of 7 μ in thickness. The effects of the surface layer on ($I_{T.D.}/I_{R.D.}$) for rolled specimens from 8 mm in thickness are shown in Fig. 12. From these figures it is clear that the orientation rotation from (110) [$\bar{1}12$] to (112) [$\bar{1}\bar{1}1$] and (110) [$\bar{3}35$]

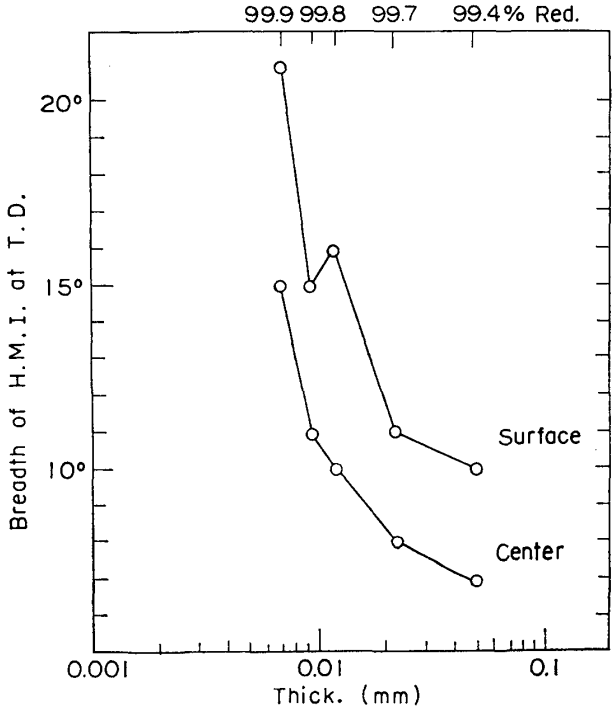

Fig. 10. Effect of cold rolling reduction and thickness on breadth of half-maximum intensities.

component is more dominant in the surface than the center layer, the (110) [112] component disappears almost and the sharp (112) [$\bar{1}\bar{1}$1] component develops in the surface layer.

Fig. 13 shows the variation of intensity distribution along the peripheral circle of (200) diffraction line for rolled sheets of 99.4 pct reduction and 50 μ in thickness and those of 99.9 pct and 7 μ in thickness in which the former has very sharp cube component and the latter has a weak cube component when annealed. The former has clearly a cube component in deformed matrix, but the latter decreases distinguishedly.

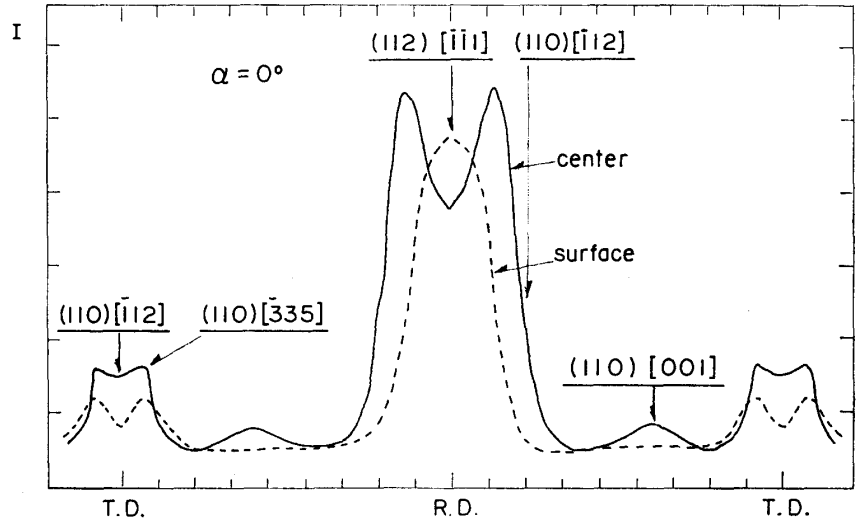

Fig. 11. Surface layer effect on variation of intensity distribution along the peripheral circle of (111) diffraction line for rolled 99.9 pct, 7 μ thickness.

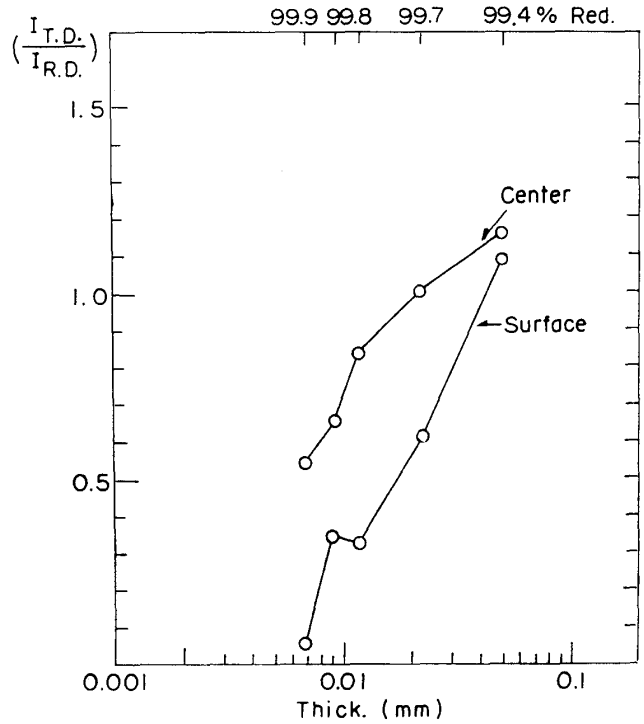

Fig. 12. Surface layer effect on ($I_{T.D.}/I_{R.D.}$) for rolled specimen from 8 mm thickness.

Table 2 shows the relation between the numbers of the recrystallized nuclei at the nucleated stage and the integrated intensity of (100) [001], existed in deformed matrix for the typical specimens, reported previously.[11]

The (100) [001] component in deformed matrix diminishes when the thickness decreases, particularly, for thickness less than 10 μ, and reduction higher than 99.4 pct and it is clear from this figure that the numbers of (100) [001] recrystallized nuclei are mutually related to the intensity of (100) [001] component in deformed matrix.

The results described above, are summarized in Fig. 14 which is a schematic diagram of cold rolling reduction and thickness effect on the intensity of each orientation component in the center layer of the specimens reduced from 8 mm in thickness.

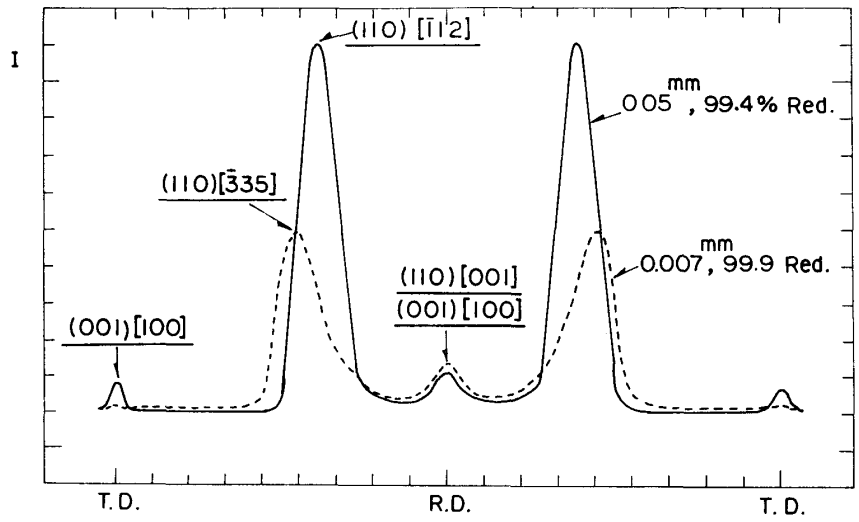

Fig. 13. Variation of intensity distribution along the peripheral circle of (200) diffraction line for rolled 99.4 pct, 50 μ thickness and 99.9 pct, 7 μ thickness.

Table 2. Relation between (100) [001] recrystallization nuclei numbers and integrated intensity of (100) [001] existed in deformed matrix.

Thick (μ)	50	20	6	7
Red (%)	99.4	99.4	99.4	99.9
I. I. (ratio)	1.0	0.98	0.83	0.33
R. Nuclei No	628	638	438	177

(11) E. Tanaka, H. Kato and T. Kondo, Preprint at the general meeting of the Japan Institute of Metals, April, 1958, p. 17.

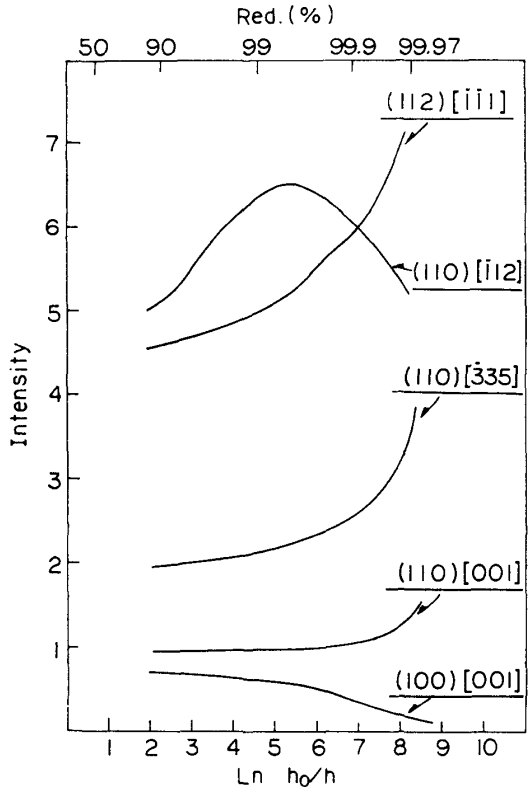

Fig. 14. Schematic diagram of cold rolling reduction and thickness effect on the intensity of each orientation component reduced from 8 mm in thickness.

IV. Discussion

It is clear from the above results that cold rolling textures of ultra-thin sheets and heavy rolled 50 pct Ni-Fe alloy under above extreme rolling condition, show peculiar textures differed from the so-called copper-type texture reported hitherto.

It is proposed below that the mechanism of texture transition and the process of formation of new orientation.

1. Texture transition of (110) [1̄12] to (112) [1̄1̄1]

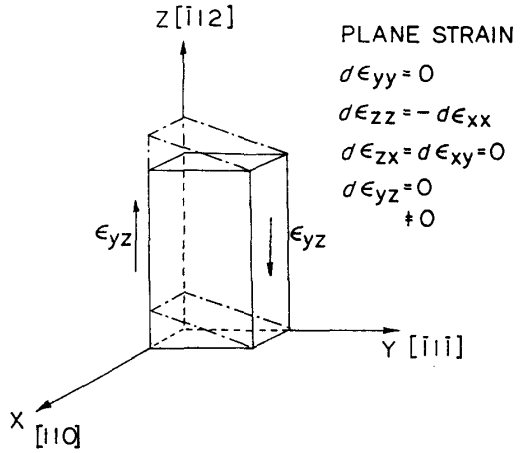

Fig. 15. Schematic drawing of (110) [1̄12] crystal on plain strain compression.

Dillamore and Roberts[2] and Smallman and Brown[3] suggested that extensive cross slip is to be responsible for the formation of copper-type texture and the texture rotates finally toward the orientation (112) [$\bar{1}\bar{1}1$] in a polycrystalline aggregate.

Fig. 15 shows the schematic drawing of (110) [$\bar{1}12$] crystal compressed on the (110) plane with the elongation confined to the [112] direction and constructed to restrict lateral spreading of the specimen. In this case the plane strain condition is as follows:[12]

$$d\varepsilon_{yy} = 0$$
$$d\varepsilon_{zz} = -d\varepsilon_{xx}$$
$$d\varepsilon_{zx} = d\varepsilon_{xy} = 0$$
$$d\varepsilon_{yz} = 0 \quad \text{or} \quad d\varepsilon_z \neq 0$$

The two favorable slip systems, (111) [101] and (111) [011], operate and hence the resolved shear stress in the cross slip systems of these two slip systems is zero on this basis. The initially rectangular geometry is changed to a paralleogram after straining in Fig. 15 and no orientation changes occur. By placing a (110) [$\bar{1}12$] crystal between rectangular polycrystalline blocks during compression, ε_{yz} is suppressed. As a result, four slip systems, (111) [10$\bar{1}$], (111) [011], (1$\bar{1}$1) [011] and ($1\bar{1}1$) [10$\bar{1}$] which are cross slip systems of the former, will operate, then no change of the initially rectangular shape occurs in the result.

However, practically the deformation in rolling for polycrystalline is not the plane strain condition, as shown above, on account of constrain of flow in the opposite direction of rolling direction, by rolls and constrain between grains, but is complex. Therefore after deformation the initial rectangular shape maintains, that is, the shear strain ε_{yz} resulting from the operation of cross slip systems, ($1\bar{1}1$) [011] and ($1\bar{1}1$) [101] for two main slip systems are suppressed, a shear stress ε_{yz} generates. By the operation of these cross slip systems, the rolling plane (110) rotates to (112) plane. In the result, the resolved shear stress in the operative slip systems, A_4 and B_4, are increasing by this rotation and the rolling direction [$\bar{1}12$] rotates to [$\bar{1}\bar{1}1$].

The cause of increasing (112) [$\bar{1}\bar{1}1$] orientation in ultra-thin sheets are considered as follows:

The center layer of the specimens in extreme thinning condition approaches to the surface layer. Cross-slip is more likely to occur in the surface[13] than the center of the sheets on account of the increasing frequency of cross slip by changing the stress system caused by friction between rolls and materials.

The mean specific roll pressures increase remarkably by thinning and the slip systems, A_4 and B_4, to be small normally, become active and (110) [$\bar{1}12$] component

(12) G.Y. Chin, E.A. Nesbitt and A.J. Williams, Acta Met., **14** (1966), 467.
(13) I.L. Dillamore and W.T. Roberts, J. Inst., Metals, **92** (1963–1964), 193.

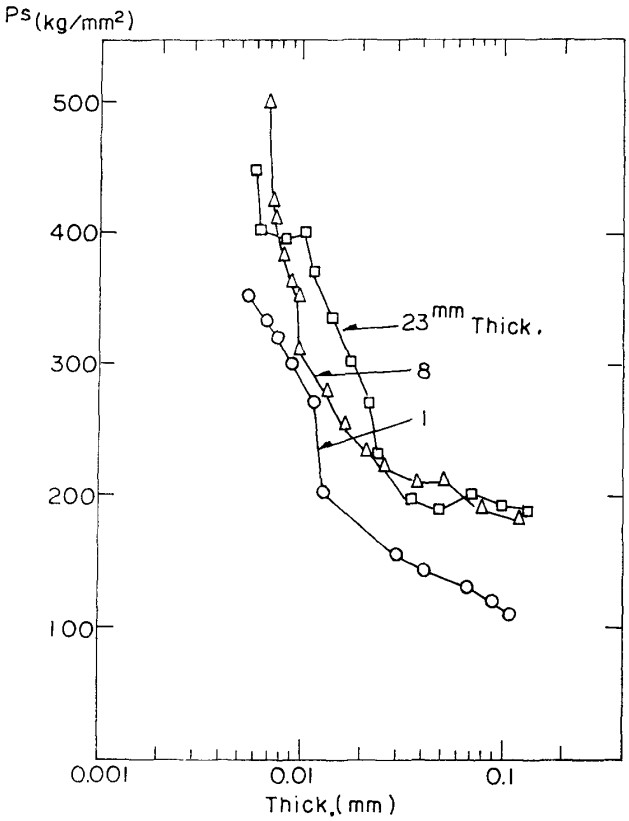

Fig. 16. Thickness effect on the mean specific rolling pressure (p_S).

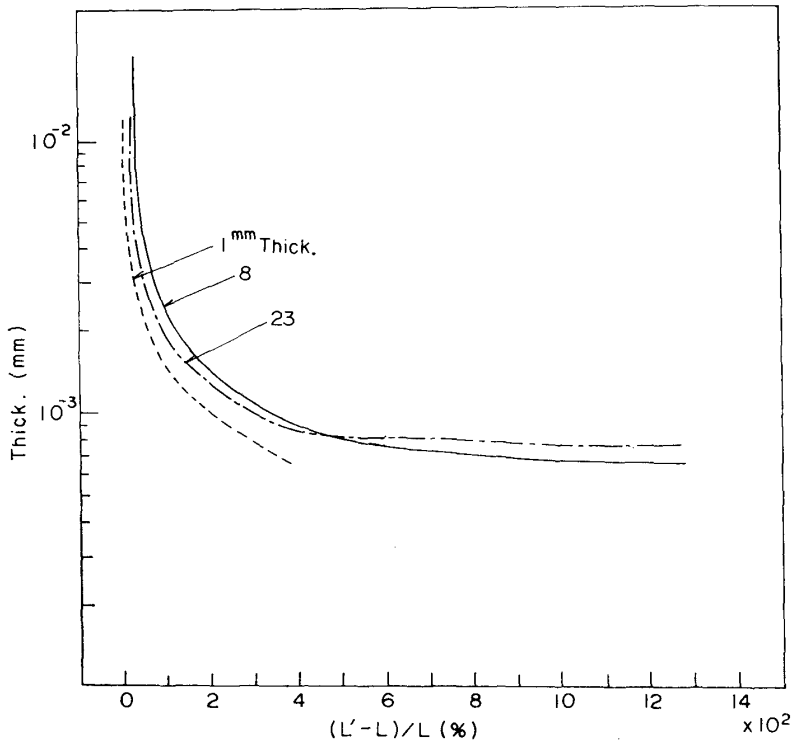

Fig. 17. Thickness effect on the roll flattening.

rotates to (112) [$\bar{1}\bar{1}1$] in the result. The thickness effect on the mean specific rolling pressure and on the roll flattening calculated by Hichcook equation[14] is shown in Fig. 16 and Fig. 17, respectively. It is clear from these results that the roll flattening and the mean specific rolling pressure increase extremely below 10 μ in thickness.

2. Formation of (110) [$\bar{3}35$]

The favoured slip systems to be main components in the (110) [$\bar{2}\bar{1}1$] orientation are A_3 and B_6. The resolved shear stress of A_4 and B_4 in the counter-clockwise direction around the normal to the (110) rolling plane is about 0.3 as compared with A_3 and B_6, that is, A_3 and B_6 are inactive in normal rolling condition. But as described above, the specific rolling pressure in the heavy rolled ultra-thin sheets becomes very large and the resolved shear stress becomes large and operative. In the result, (110) [$\bar{2}\bar{1}1$] rotates to (110) [$\bar{3}35$] orientation.

3. Existence of (100) [001] in deformed matrix

The (100) [001] in deformed matrix in rolled Fe-Ni alloys has been found in several reports.[4),(15),(16)]

It is very interested that the numbers of (100) [001] recrystallized nuclei are mutually related to the intensity of (100) [001] component in deformed matrix. The fact of the remarkable decrement of the (100) [001] recrystallized nuclei in spite of increment of twin related {112} ⟨111⟩ rolling texture in the ultra-thin and heavy rolled sheets, is thought to deny the inverse-Rawland[17] mechanism.

The details of the origin of recrystallization textures in these specimens will reported in next report.[18]

Acknowledgements

The authors wish to express hearty thanks to Mrs. R. Katuta and Miss S. Inomata for assisting the analysis and the adjustement of experimental data.

(14) L.R. Underwood, *The Rolling of Metals*, Chapman and Hall, p. 170.
(15) H. Abe and H. Seki, J. Japan Inst. Metals, **23** (1959), 343.
(16) H. Nakae and A. Okada, J. Japan Inst. Metals, **32** (1968), 368.
(17) C.A. Verbraak, Acta Met., **5** (1957), 765.
(18) H. Kato and E. Tanaka, Preprint at the general meeting of the Japan Inst. Metals, March, 1969. p. 121, 122.